Journal of ELECTRICAL ENGINEERING, VOL 71 (2020), NO2, 110–115

PAPER

A hairpin DGS resonator for application to microstrip lowpass filters

Rong-Bin Chen[1], Xiao-Ou Ou[2]

A hairpin shaped DGS, consisting of two tilted slots with a separation angle, is studied as a unit cell in this contribution. It is further served as a microwave resonator for microstrip lowpass filter applications. Two prototype filters that respectively cascade the same unit cells and the scaled cells with a different scale ratio are analyzed. For demonstration purposes, the two prototype filters are optimally developed, fabricated and examined both from numerical simulations and from experimental validations. Results show the cascaded scaled type demonstrator features a high stopband suppression level within a wide frequency band.

K e y w o r d s: defected ground structure (DGS), hairpin, lowpass filter, microstrip

1 Introduction

Microwave filters and the filter based components are indispensable in many telecommunication electronics and have found wide applications in signal filtering and selecting [1–6], time reversal super resolution transmission [7] and imaging just to mention a few. The introduction of geometrical patterns or shapes etched off on the metallic ground plane of microstrip based filter implementation has been demonstrated good probabilities for filter designs due to its ability to vary the frequency responses of the structure. The defected ground structure (DGS) implementation of microwave filters is a good choice for the purpose to realize low profile compact filters without compromising the achieved performance [8–20]. Conventional microstrip lowpass filters have been developed using shunt stubs [2], or high-low-high impedance transmission lines [8]. For such configurations, a sharp roll-off corresponds to multi-stage high-low-high impedance sections that could result in drastic increase in circuit size. This calls for methods in lowpass filter designs to realize estate size reduction but without sacrificing the performance.

Studies indicate a way to reduce the circuit size can be by integrating the slow-wave phenomenon [3]. In [15], a patterned microstrip line is studied, where complementary rectangle split ring resonator is introduced to approach slow-wave effect, and further by introducing the dumbbell-shaped DGS to improve the filter performance. By embedding several U-shaped DGS together, isosceles U-shaped DGS is developed, where owing to the embedded architecture, size reduction could be approached [16]. On the other hand, the transition skirt from the passband to the stopband is also critical for microwave filter applications since such a term represents the filter selectivity. To improve the transition skirt or achieve a sharp roll-off, double E shaped DGS [17] and interdigital DGS [18] are proposed. Results indicate such kind of structures can introduce an attenuation pole that is close to the cutoff frequency, thus greatly enhancing the transition rate. Moreover, studies show the reflection pole can also be generated near the cutoff frequency, which improves the passband insertion loss and yields a flat passband. Another issue related to the microwave filter is the stopband responses. In general, the spurious passband is unavoidable as a result of the periodic response characteristics of microwave transmission lines. Hence a wide stopband with high suppression level is appreciated in practical engineering. Studies indicate using cascaded multi-stage DGS can result in a widened stopband, as presented in [19]. Meanwhile, this purpose can also be achieved by introducing some optimal methods, as reported by Boutejdar and Bennani [20].

In this contribution, a hairpin shaped DGS is studied. It constitutes a pair of slots that are tilted placed with a separation angle of α. For microwave filter applications of such a kind of DGS, two prototype microstrip lowpass filters, by cascading the same unit cells and the scaled cells with a scale ratio of ρ, are respectively discussed and developed. Demonstrations on the two fabricated prototypes show expected responses, both from numerical simulations and from experimental examinations. For the developed two prototypes, both exhibit sharp transition skirt, while for the one by cascading the scaled cells, a wide stopband with high suppression level is observed, thus making it attractive for potential applications in microwave engineering.

[1] Department of Electronic and Information Technology, Jiangmen Polytechnic, Jiangmen 529030, China, chenrongbin@139.com,
[2] Jiangmen Branch, China Mobile Group Guangdong Co., Ltd., Jiangmen 529000, China, ouxiaoou2@gd.chinamobile.com

DOI:10.2478/jee-2020–0016, Print (till 2015) ISSN 1335-3632, On-line ISSN 1339-309X

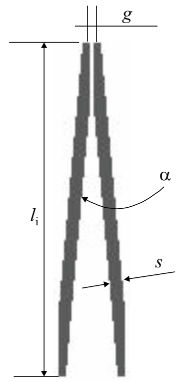

Fig. 1. Basic configuration of the hairpin DGS

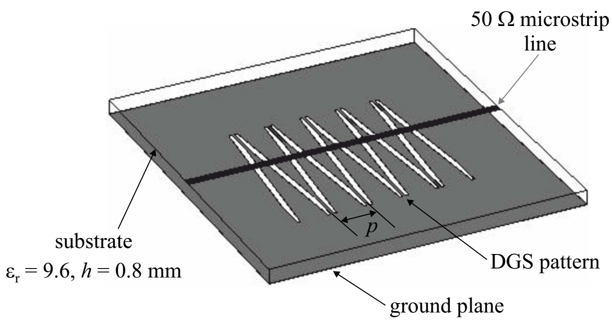

Fig. 2. 3D view of the lowpass filter(type a)by cascading unit cells with a periodicity of p

2 Hairpin DGS architecture and its application to microstrip lowpass filters

Figure 1 shows the studied hairpin DGS. It consists of two tilted slots with a separation angle α. The two tilted slots have a height of l_i and the separation at the closed apex is marked as g, where the subscript i deq notes the order number when it is further cascaded. Meanwhile, each slot has width of s. The architecture is etched off on the back metallic ground side of a microstrip transmission line. The patterned defects on the metallic ground plane distracts the current distributions, resulting in the alterations of the transmission line properties and thus creating the slow-wave effect and realizing the band rejection property [13]. In general, the slot resonates at a half wavelength, thus it determines the center frequency of its transmission and reflection responses when dedicated to microwave filter applications.

2.1 Microstrip filter type A (directly cascading unit cells with the same size)

Figure 2 presents the 3D view of the discussed hairpin DGS lowpass filter, where five basic hairpin DGS cells are cascaded uniformly with the same size and a periodicity of p. The microwave substrate utilized here has a relative permittivity of $\varepsilon_r = 9.6$ and a thickness of $h = 0.8$ mm. On the top side of the substrate, a microstrip transmission line is considered that has a line width of 0.76 mm for a 50 Ω system.

The structure shown in Fig. 2 is numerically analyzed by parameter sweeping. The full-wave electromagnetic (EM) simulator, Ansoft Ensemble 8, is employed to carry out the EM analyses. In the sweeping studies, we set the parameter g to be constant as 0.2 mm. The initial height $l_i = 20$ mm and the separation angle $\alpha = 10°$. Figure 3(a) shows the sweeping results for respectively $\alpha = 10°$ and 12° under $l_i = 20$ mm. Notice that for clarity, only two groups' results are illustrated in the Fig.3. It is seen from Fig. 3(a) that increasing α corresponds to increasing the slot length and therefore, the resonance shifts to the lower frequencies. Here the 3 dB cutoff frequency is 3.32 GHz and 3.29 GHz for $\alpha = 10°$ and 12° respectively. Further, decreasing the height l_i to 18 mm is studied, as described in Figure 3(b). Clearly, this formulates the reduced slot length and thus the resonance would shift to the higher frequencies. In this study, the 3 dB cutoff frequencies are respectively located at 3.685 GHz and 3.61 GHz under $\alpha = 10°$ and 12°.

Also, the effect of the slot width on its performance is parameter swept. Figure 4 plots the simulated results. It is observed from the Figure that the slot width would slightly influence the return loss of the five cascaded cells under the different cases for $s = 0.5$ mm, 0.7 mm and 1.0 mm. This is because the slot width formulates the characteristic impedance of a slot line on a given microwave substrate, and further describes the impedance matching between the microstrip line and the slot.

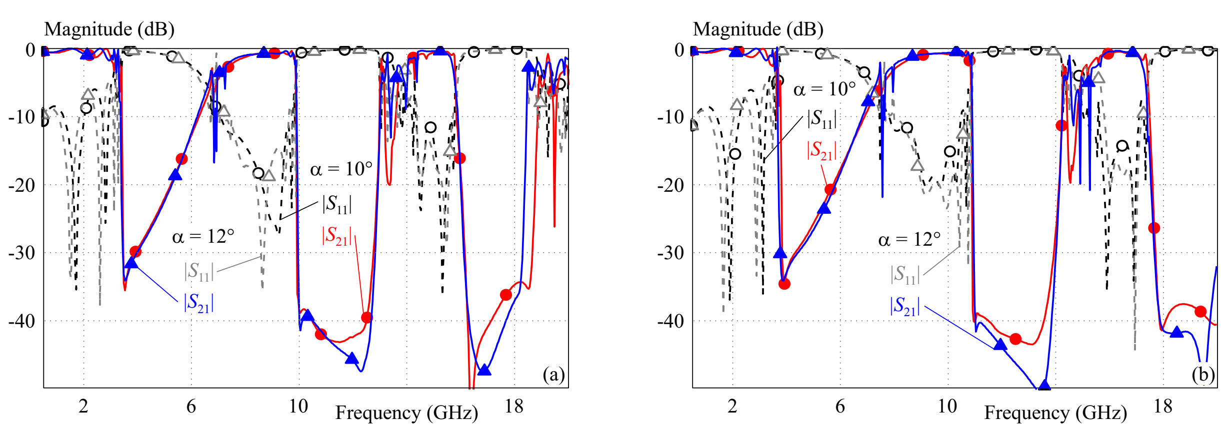

Fig. 3. Sweeping results for different separation angle α for: (a) – $l_i = 20$ mm, and (b) – $l_i = 18$ mm

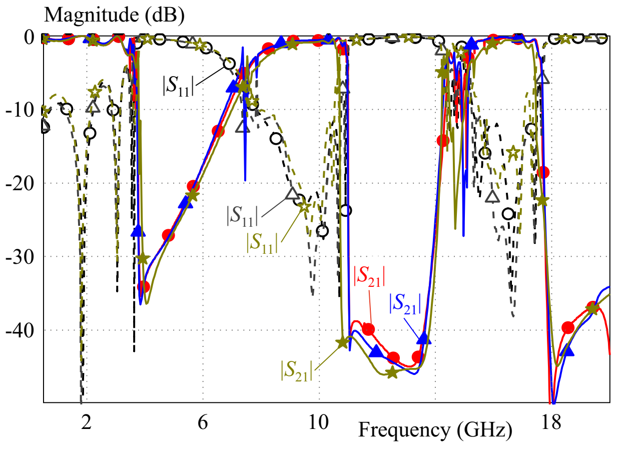

Fig. 4. Parameter sweeping study on the slot width, where the triangles denote $s = 0.5$ mm, the circles represent $s = 0.7$ mm and the pentagrams stand for $s = 1.0$ mm

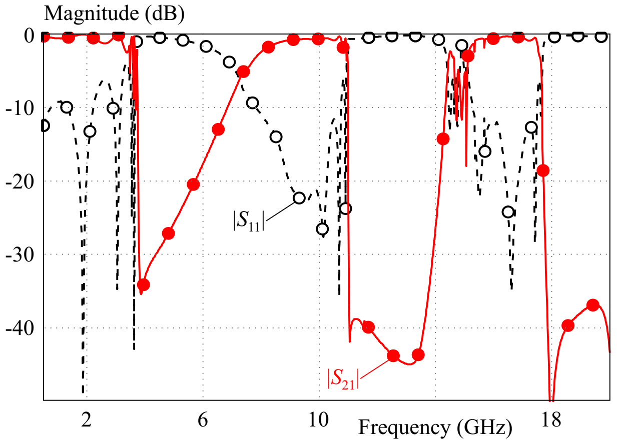

Fig. 5. Simulated S parameters of the lowpass filter (type A)

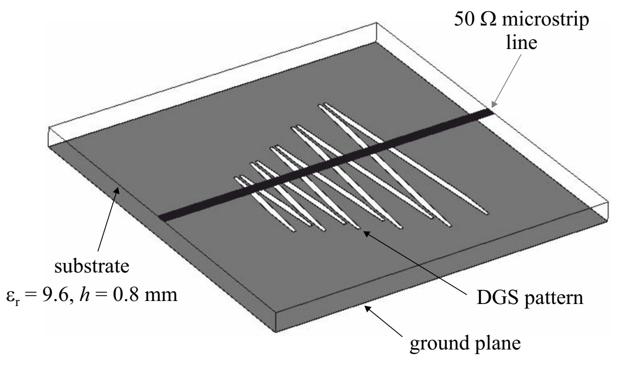

Fig. 6. 3D view of the studied lowpass filter(type B) by cascading the scaled unit cells

2.2 *Microstrip filter type B (cascading scaled unit cells with a scale ratio of* $\boldsymbol{\rho}$

Figure 6 shows the 3D view of the improved filter (type B) by cascading scaled unit cells. Also, five cells are studied here, and the scale ratio is defined as

$$\rho = \frac{l_{i+1}}{l_i}, \qquad i = 1, 2, 3 \ldots \tag{1}$$

where l_i is the height of the hairpin DGS shown in Fig. 1.

This cascaded scaled structure is also parameter sweeping study to characterize its performance. Here, we primarily focus on the influence of scale ratio ρ on the frequency responses, meanwhile, studies indicate similar responses compared to the above Sub-section are found for other parameters. Figure 7 presents the simulated S parameters under three different ratios. It is seen for a smaller ratio of $\rho = 0.7$, the near stopband (namely close to the 3 dB cutoff frequency) has a strong resonance (exhibiting as a transmission peak) at approximately 4.5 GHz. When increasing the ratio ρ, the structure will gradually approach to the standard case as discussed on the above Sub-section; for instance, when $\rho = 0.9$, it is found strong spurious passband occurs near at 10 GHz. This means if a suitable stopband suppression is appreciated for microwave lowpass filter applications, optimal determination on such a ratio is important.

Based on these discussions, a microstrip lowpass filter with sharp transition from the passband to the stopband and wide stopband suppression is designed, where the desired 3 dB cutoff frequency is set to 3.5 GHz and up to 20 GHz, the desired suppression should be as high as possible. The microwave substrate utilized is the same as mentioned before.

The filter (type B) is optimally developed using the above same EM simulator. Figure 8 presents the frequency responses for the final determined parameters. It is seen the filter behaves sharp transition shirt and a wide stopband suppression level. Also it is mentioned that some extra resonances (exhibiting as the reflection notches) at approximately 13 GHz, 15 GHz and 16 GHz with good transmission suppressions are due to the EM radiations since the patterned slots function as antennas under open free space. This phenomenon can be mitigated by attaching another grounded substrate or put the structure into a metallic cavity.

The EM optimized dimensions of such a filter are: $g = 0.2$ mm, $\alpha = 10°$, $l_1 = 18.4$ mm, $l_2 = 15.272$ mm, $l_3 = 12.676$ mm, $l_4 = 10.521$ mm, $l_5 = 8.417$ mm, and $s = 0.55$ mm. Also, the microstrip line width of 0.76 mm describes a characteristic impedance of 50 Ω. The filter has a corresponding scale ratio of $\rho = 0.83$, and the total size is 14.85 mm × 18.4 mm.

3 Experimental validations on the above developed filters

The above developed two prototype filters (namely type A and type B) are fabricated to further experimentally characterize the achieved electric performance. Measurements are carried out by using a vector network analyzer, N9918A, with full two-port calibrations.

Shown in Fig. 9 is the photograph of the fabricated filter type A. The measured results are recorded in Fig. 10.

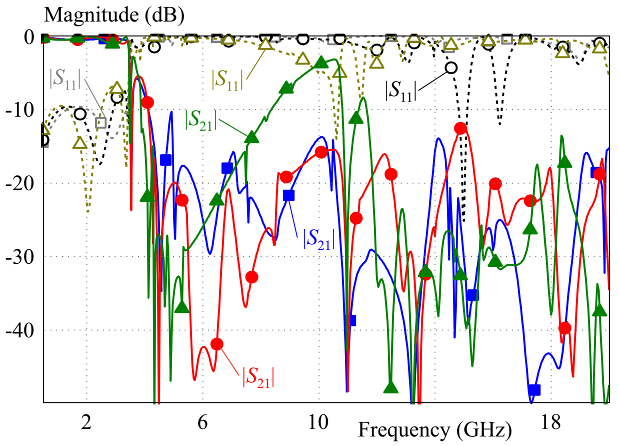

Fig. 7. Sweeping results of the filter type B, where the squares correspond to the scale ratio $\rho = 0.7$, the circles stand for $\rho = 0.8$, and the triangles represent $\rho = 0.9$

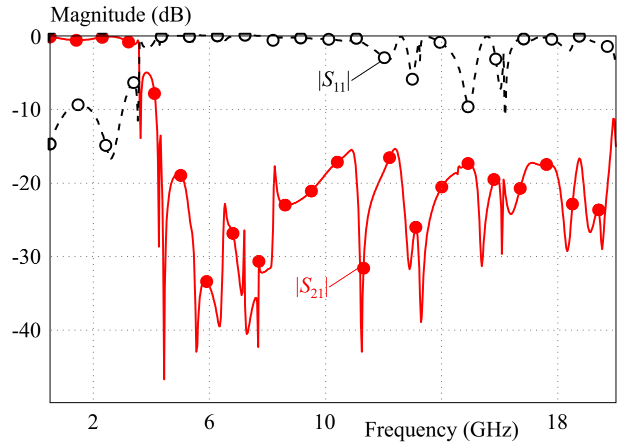

Fig. 8. Simulated frequency responses for the studied lowpass filter (type B

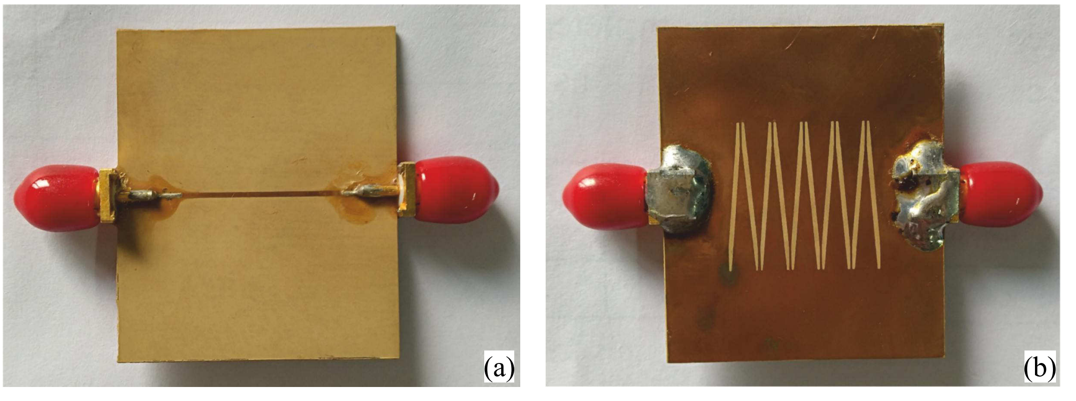

Fig. 9. Photograph of the fabricated filter type A: (a) – the front side, and (b) – the back side

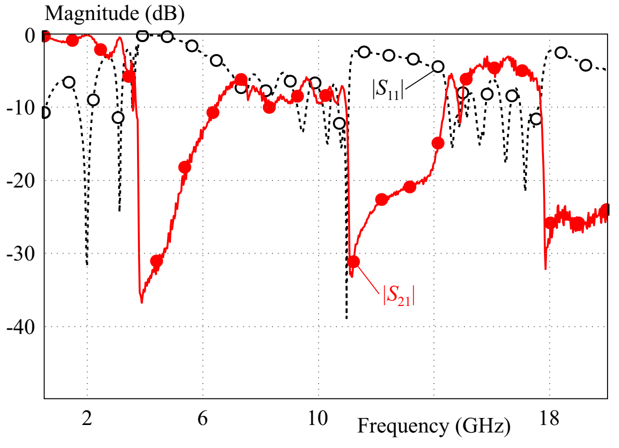

Fig. 10. Measured frequency responses of the fabricated filter type A

As expected, periodic resonances are found from measurements and therefore, it has poor stopband suppressions, but a sharp transition from the passband to the stopband at approximately 4 GHz is observed. As compared to the simulations shown in Fig. 5, similar responses can be seen and the slightly higher loss in the passband is attributed to the two back-to-back transitions between the microstrip line and SMA connectors as well as the dielectric and strip losses. Meanwhile, the simulated in-band matching is not so good that also contributes to the higher return loss from measurements.

Figure 11 shows the photograph of another fabricated filter type B. Measurements indicate that the demonstrator has an in-band insertion loss of 0.45 dB in general from DC to 3.1325 GHz, and the 3 dB cutoff frequency is approximately 3.62 GHz. The first transmission zero is located at 3.9125 GHz with a level of -16.1 dB that also depicts a sharp transition from the passband to the stopband. From 4.4488 GHz to over 20 GHz, the suppression level is better than 16.6 dB. Also, as discussed above, owing to the open free space of the DGS pattern, the slots at some frequencies act as EM radiators and thus radiate EM energy into the open free space. Consequently, the measured return loss at the stopband exhibits several notches within the band of interest. Due to the use of scaled unit cells, a wideband suppression is achieved as compared to the filter type A.

When compared the measurements shown in Fig. 12 and the simulated performance given in Fig. 8, one can

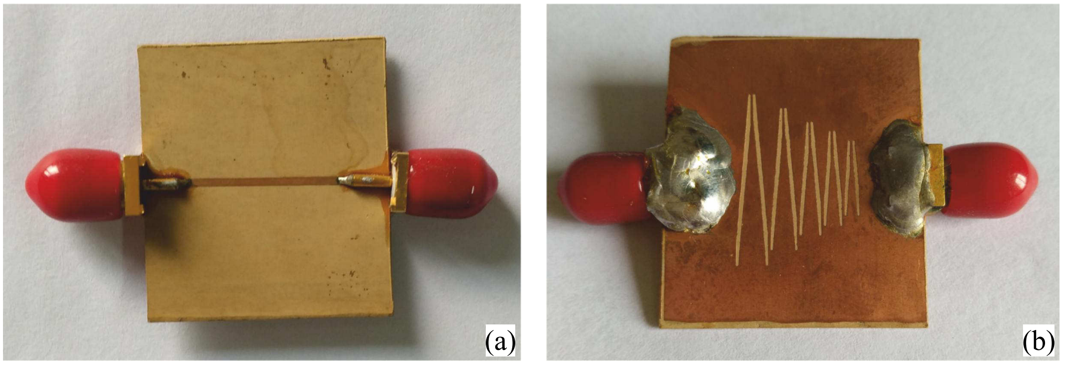

Fig. 11. Photograph of the fabricated filter type B: (a) – the front side, and (b) – the back side

Table 1. Performance comparisons of some related published works and this study for type B

Refs/Year	$f_{c3\,dB}$ (GHz)	First attenuation pole/level	Stopband range /suppression level	Filter size* (mm^2)	Notes	ε_r	h (mm)
[15]/2017	3.88	44.35 dB/4.14 GHz	20 dB/4.07 15 GHz	35.25 × 16.15	Patterned microstrip and dumbbell-shaped DGS	2.55	1.5
[16]/2017	14.2	57 dB/15.8 GHz	22 dB/10 30 GHz**	14.44 × 3.4	Isosceles U-shaped DGS	2.2	0.7874
[17]/2012	2.7	62 dB/3.66 GHz	35 dB/3.39 7.37 GHz	27 × 7	Double E shaped DGS	9.6	0.8
[18]/2015	3.11	22.5 dB/3.23 GHz	25 dB/3.24 ≈ 10.7 GHz	20.02 × 13.64	Interdigital DGS	10.2	1.27
[19]/2016	1.49	57.2 dB/2.0 GHz	20 dB/1.65 7.41G	40 × 20	Fan-shaped DGS and double radial stub	10.2	0.635
[20]/2017	4.0	32.81 dB/6.7 GHz	20 dB/4.3 20 GHz**	50 × 14	Cross shaped DGS	3.38	0.813
This work	3.62	16.1 dB/3.9125 GHz	16.6 dB/4.4488∼> 20 GHz	14.85 × 18.4	Hairpin shaped DGS	9.6	0.8

*determined by length × width **from simulations

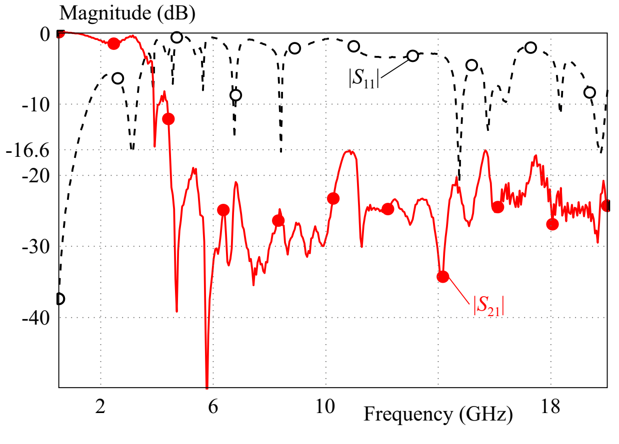

Fig. 12. Measured responses of the fabricated demonstrator filter type B

see good agreement can be found, thus validating the effectiveness of this study.

Further, Tab. 1 lists some published DGS based microwave lowpass filters and our developed lowpass filter type B for performance comparisons. It is seen that in general, the developed prototype demonstrator type B could characterize a relatively high suppression level within a very wide stopband, and a compact occupied filter area. Moreover, the studied DGS is very simple in structure, as compared to other reported results are Tabulated.

4 Conclusions

A compact hairpin shaped DGS is introduced and discussed for microwave filter applications. The studied DGS characterizes simple architecture, and can generate attenuation pole and reflection pole near the cutoff frequency. For microstrip lowpass filter demonstrations, studies show a wide stopband with high suppression level can be approached by using cascaded scaled cells. Experimental examinations on the developed prototype filters validate the predications well, thus confirming the study of this contribution. It is believed the presented DGS is attractive for further integrated with other microwave circuits, components or modules for system applications.

References

[1] X.-B. Zhang, J.-L. Li and S.-S. Gao, "Analysis on Transmission Zeros Cross-Coupled Microstrip Filters", *Electromagnetics*, vol. 37, no. 2, pp. 81–91, Mar 2017.

[2] J.-L. Li, S.-W. Qu and Q. Xue, "Compact Microstrip Lowpass Filter with Sharp Roll-Off and Wide Stop-Band", *Electronics Letters*, vol. 45, no. 2, pp. 110–111, Jan 2009.

[3] J.-L. Li, W. Shao, J.-P. Wang, X.-S. Yang and S.-S. Gao, "Microwave Slow-Wave Structure and Phase-Compensation Technique for Microwave Power Divider", *Radio Engineering*, vol. 23, no. 1, pp. 214–221, Apr 2014.

[4] B. A. Twumasi, J.-L. Li and L. Xia, "A Multi-Coupled Line Based Microstrip Diplexer with High Figure-of-Merit", *Electromagnetics*, On-line.

[5] J. Zhou, J.-L. Li, C.-G. Sun, H. Li and S.-S. Gao, "A Novel Microstrip Diplexer Based on Coupled Line", *Electromagnetics*, vol. 38, no. 2, pp. 87–95, Mar.2018.

[6] B. A. Twumasi and J.-L. Li, "A Compact, Wideband Branch-Line Balun with Small Magnitude and Phase Imbalances", *Electromagnetics*, vol. 39, no. 1, pp. 30–40, Feb 2019.

[7] B. A. Twumasi and J.-L. Li, "Numerical Simulation Study on Bowtie Antenna-Based Time Reversal Mirror for Super-Resolution Target Detection", *Journal of Electrical Engineering*, vol. 70, no. 3, pp. 236–243, June 2019.

[8] M. Chetioui, A. Boudkhil, N. Benabdellah, A. Kafi and N. Benahmed, "A New Design of Quasi-Elliptic High-Low Microstrip Lowpass Filter using SC-Defected Ground Structure Technique", *15th International Multi-Conference on Systems*, Signals & Devices, 2018, pp. 425–428.

[9] B. A. Twumasi and J. -L. Li, "An Equivalent Circuit Model of a Rectangular Bracket Shaped DGS and its Microwave Filter Applications", *Journal of Electrical Engineering*, vol. 70, no. 1, pp. 32–38, Feb 2019.

[10] M. Berka, Z. Mahdjoub and M. Hebali, "New Design of Dual-Band Bandpass Microwave Filter Based on Electromagnetic Effect of Metamaterial Resonators", *Journal of Electrical Engineering*, vol. 69, no. 4, pp. 311–316, Aug 2018.

[11] W. Shao and J.-L. Li, "Design of a Microwave Frequency Triplr with Conversion Gain", *Journal of Electromagnetic Waves and Applications*, vol. 26, no. 2/3, pp. 226–238, Jan 2012.

[12] B. T. P. Madhav, S. Rajiya, B. P. Nadh and M. S. Kumar, "Frequency Reconfigurable Monopole Antenna with DGS for ISM Band Applications", *Journal of Electrical Engineering*, vol. 69, no. 4, pp. 293–299, Aug 2018.

[13] E. K. I. Hamad and A. Abdelaziz, "Metamaterial Superstrate Microstrip Patch Antenna for 5G Wireless Communication Based on the Theory of Characteristic Modes", *Journal of Electrical Engineering*, vol. 70, no. 3, pp. 187–197, June 2019.

[14] H. Fu and Y. Yu, "A Novel Lowpass Filter Based on Multistage Defected Ground Structure", *IEEE International Conference on Ubiquitous Wireless Broadband*, 2016, pp. 1–4.

[15] P. Zhang and M. Li, "A Novel Sharp Roll-off Microstrip Lowpass Filter with Improved Stopband and Compact Size using Dual-Plane Structure", *Microwave and Optical Technology Letters*, vol. 58, no. 5, pp. 1085–1088, May 2016.

[16] B. Sahu, S. Singh, M. K. Meshram and S. P. Singh, "Defected Ground Structure Based Compact Microstrip Lowpass Filter with Wide Stopband", *IEEE Applied Electromagnetics Conference*, 2017, pp. 1–2.

[17] W. Shao and J. -L. Li, "Accurate Modeling of a Patterned Ground and its Application to Microwave Filters", *Applied Computational Electromagnetics Society Journal*, vol. 27, no. 7, pp. 596–602, July 2012.

[18] S. Liu, J. Xun and Z. Xu, "Sharp Roll-off Lowpass Filter using Interdigital DGS Slot", *Electronics Letters*, vol. 51, no. 17, pp. 1343–1345, Aug 2015.

[19] A. O. Ertay, M. Abbak and S. Simsek, "An Improved Stopband and Sharp Roll Off Microstrip Lowpass Filter with Defected Ground Structures", *International Journal of Microwave and Wireless Technologies*, vol. 8, no. 3, pp. 573–581, Mar 2016.

[20] A. Boutejdar and S. D. Bennani, "Improvement of lowpass and Bandpass Filter Characteristics using Cross-DGS-Resonators, Logarithmic Series and Coupling Matrix Methods", *International Conference on Wireless Technologies*, Embedded and Intelligent Systems, 2017, pp. 1–6.

Received 22 August 2019

Rong-Bin Chen was born in January 1980 at Guangdong, China. He received BS Degree from the Shantou University, Shantou, China, in 2003, and MS Degree from the Sun Yat-sen University, Guangzhou, China, in 2005. From July 2005 to June 2018, he was with the Jiangmen Branch of China Mobile Group Guangdong Co., Ltd., Jiangmen, China, where he served as a Technique Supporter for maintenance, construction and development of 2G/3G/4G/5G wireless/mobile networks. Since June 2018, he has been with the Department of Electronic and Information Technology, Jiangmen Polytechnic, Jiangmen, China. His research interests include wireless communication technology, internet of things, and so on.

Xiao-Ou Ou was born in March 1981 at GuangXi, China. She received BS Degree from the Shantou University, Shantou, China, in 2003, and MS Degree from the Sun Yat-sen University, Guangzhou, China, in 2006. From July 2006 to now, she was with the Jiangmen Branch of China Mobile Group Guangdong Co., Ltd., where she served as a Technique Supporter for business. Her research interests include Communication and information technology.